.

VLT ALL SKY IMAGER
- first ideas for implementation

H.Pedersen, M.Sarazin, A.Wicenec, C.Cavadore

Draft, June 25, 1999

1 Introduction

Most VLT observations will be made under conditions, where the observer can not ascertain the quality of the night sky without risking the loss of observing time. It therefore seems reasonable to equip the VLT with some sort of sky monitor [1]. This would function in conjunction with other environmental measurements already in progress. Amongst these is a new service introduced at ESO to forecast cloudiness and water vapor from satellite images [2]. Not only the VLT, but also other telescopes at Paranal will benefit, in particular NAOS (1st light end 2000) and VST (2001).

While a commercial CCD system has already been procured, this will primarily assist VLT operations by presenting an image of the sky, from which the observer can infer the presence of clouds by visual inspection. For the quantitative assessment of cloud cover, sky brightness, and the more ambitious measurement of (multicolor) extinction, a proper image analysis system is required. This will also be needed to monitor a number of other effects, which influence observing conditions at Paranal [3]. We envision that the VLT All Sky Imager (ASI) will perform:

- Quantitative assessment of cirrus cover to $20'$, 30 second resolution, 1% accuracy; presentation of contour maps, with possibility for time-compressed replay;
- Measurement of B, V, R extinction coefficients to $2°$, 5 minute resolution, 0.5% accuracy;
- Measurement of moon-lit sky background to $2°$, 5 minute resolution; presentation of contour maps, with possibility for time-compressed replay;
- Detection of aircraft, satellites, meteors, and logging of their closest approach to VLT UTn;
- Detection of jet aircraft contrails; prediction of crossing moments over VLT UTn field-of-view;
- Generate nightly log files (transparency, sky brightness, etc., for individual UTn), and data for statistical analysis of observing conditions.

Although there appears to be a general consensus that such quantitative information is desirable, there is no easy way of optimizing system parameters. It may therefore be reasonable to investigate what can be achieved by devices, computing power and software already available or expected to become available within approximately one year. It should then be asked, if the performance of that system will be of value to the Paranal operations, or if a more ambitious set-up is needed.

Concurrent with this discussion, it might be investigated, if the system will be capable (still within reasonable costs in software development), to produce science of its own. This can be through the scheduled monitoring of known objects, or the discovery of new photometric variables, as well as objects with large proper motion (comets, asteroids, near-earth objects).

We have investigated if any suitable system is already in use, and commercially available. Indeed, "All Sky Imagers" are in use on many sites, partly for aeronomical purpuses, partly for astronomical. Some of the more interesting are the systems built by the Atmospheric Optics Group of the Scripps Institution, San Diego [4], and by Boston University, for McDonald Observatory [5]. However, these, and most others we are aware of, are based on image intensifier tube technology. It is our impression that they do not have the resolution and photometric accuracy required to solve the above issues.

2 Field of view

The base-line for the present discussion is the wish that zenith distances less than 60°, corresponding to the typical VLT operating zone, shall be mapped, if not the entire visible hemisphere. This can either be done through a single optical system, or by a small array of cameras, most likely 2 x 2 cameras, pointing some 30-40° off zenith, imaging four quadrants of the sky. Fish-eye lenses are disfavoured for their low equivalent aperture. It has also been pointed out that a zenith-centered system is desirable, since most VLT observations are expected to be conducted near zenith.

In the following, we shall explore the possibilities of a single field-of view, of maximum extent 90°. We shall anyhow refer to this as the VLT All Sky Imager, or ASI.

One particular concern relates to the presence of very bright objects in the field-of-view. These will produce saturation of the chip charge wells. Unless the CCD is equipped with anti-blooming gates, charge-spill will affect many rows above and below each such object. Anti blooming capabilities vary from 100 to 10,000 times the saturation magnitude according to the chip characteristics. Whether or not the full Moon or bright stars will still produce charge overflow patterns depends on the f-ratio of the optical system, and its image definition. The full Moon, furthermore, will produce scattered light in the optics, interfering with measurements of the sky background. Operation of a lunar-occultor, a 'shadowing finger', is troublesome, and shall be avoided, if possible.

3 CCD detector

As with almost any CCD detector for astronomy, high pixel number, and high quantum efficiency is of paramount importance. For the present application multiple ports and/or quick read-out are also important, as are other parameters. In Table 1, we summarize the properties of the large-format chips currently available to ESO. Readout noise is not addressed as it depends strongly on readout speed.

Many of these devices are 2 k x 4 k, mostly three side buttable, and some 2 k by 2k or 4 k by 4k. While intended for other use, their size appears reasonable for use as detector in an ASI, in particular if assembled into square devices. Being back-side illuminated, these chips have high quantum efficiency and are not equipped with anti-blooming gates.

The largest chip currently available at ESO is the 7 k x 9 k (7168 x 9216 pixel) Philips chip.[51][38] Two of these have been acquired, of which one is currently on loan to Observatoire de Cote d'Azur. The chip has antiblooming gates superimposed. The relatively low quantum efficiency, 13 % at 420 nm, 27 % at 530 nm, and 7% at 800 nm, is inherent to the performance of front-side illuminated devices having anti-blooming gates. The chip can be read through four amplifiers simultaneously. Using the ESO CCD controller FIERA, the rate is up to 1 Mpix/second, but ongoing developments aim to increase this to 2 Mpix/second. The corresponding read-out noise is 10 e^-. The chips have specular reflectivity near 5%, which may add to internal reflexes in the optics. One further concern relates to the non-uniform sensitivity across any single pixel. This is caused by the partially non-transparent nature of the anti-blooming gates.

An even larger detector (in pixel number) is the recently announced 9 k x 9k Lockheed-Martin chip. Like the Philips chip, it is front-illuminated. Although by no means assuming that this will become available in the near future, we shall in the following take its properties as an example of what can be reached, if indeed mounted in a VLT-ASI.

Chip name	Area pixels	Pixel μm	QE % @420/530/800 nm	Qmax ke-	On Chip A-blooming vert. Qmax *i*	MPP yes/no *ii*	Readout Mpx/s/port (ports) *iii*	Cost Pf./px
Lockheed-Martin	9k x 9k	8.75	*iv*	100	no	??	25 (tbc) (8)	n.a.
Philips	7168x9216	12	13/27/7	200	200	no	5 (4)	N/A
Kodak (kaf 16807)	4096x4096	9	7/30/42 32/50/30	80	no	yes	20 (1)	?
EEV	2048x4096	15	85/87/57	300	no	no	1 (2)	?
Lincoln Lab	2048x4096	15	25/65/80	200	no	no	1 (2)	?
SIte SIte	2048x4096	24	60/75/65	150 350	no	yes no	1 (4)	?
Loral	2048x2048	20	75/93/90	150	no	yes	0.1 (4)	0.5
TH7899M	2048x2048	14	7/18/35	200	no	yes	20 (4)	0.175
VLT-TCCD	576x576	22	20/50/?/	200	no	no (2.5Φ)	0.5 (1)	4.5

Table 1: Full Frame Detector List

Notes:

i With antiblooming gates, the sensitivity profile across the pixel is not constant, as a fraction of the area is lost. This implies a reduced quantum efficiency. By means of image phase clocking during integration, chips without antiblooming gates can be operated in a manner which inhibits blooming.

ii MPP is a chip fabrication process which permits to achieve low dark current at non-cryogenic ambient temperature (this may cause decreased MTF).

iii Readout speed: current ESO FIERA CCD controllers limit the readout speed to 1 Mpix/s/port

iv Quoted as > 35 % from 550 to 800 nm.

4 Optics

A provisional study, kindly made by Mr. Blechinger of Rodenstock Präcisionsoptik, gives the performance of a F=20 mm, f/3.5 (effective), 90° (diagonal) lens, optimized for use with a 4k x 4k CCD of resolution 12.5 μm. The lens is apochromatic from 400 - 1000 nm. At the center of the field, the sagittal and tangential modulation transfer function (MTF) is about 80% for 20 line pairs per millimeter, decreasing to 35%, at the edge. This means that stars will be spread over typically ~4 x 4 pixels. This degree of oversampling is desirable, for high-precision photometry. The apochromatic lens will permit the successive use of several wide-passband filters, hence deduction of color-dependent extinction coefficients.

In the following, we shall assume that the design can be scaled upwards in focal length, to F = 80 mm, while maintaining resolution at the somewhat slower ratio f/4.5 (effective). This is justified by the relaxation of some design criteria, which are not relevant for astronomical lenses: back-focal distance, distortion, and apochromacity. As to the latter issue, one should consider that the optics (almost) exclusively will be used with astronomical color selection filters, B, V, R, typically 120 nm wide. Focus adjustments between exposures will care for most of the chromatic effects, and some of the remainder can be compensated by proper optical design of the color-filters.

5 Operation

5.1 Location at Paranal

In its ultimate scope, the ASI should have the same field-of-view as the sum of all telescopes at Paranal, i.e. the entire sky. Unless mounted on a specially constructed tower, no location can provide this sky coverage. Alternatively the horizon should be reasonably free, in particular to the West from where most disturbances originate. It should also be up-wind from traffic (which cause dust accumulation), and well protected against man-made light contamination. Ease of service is an argument, which calls for a location jointly with other monitors (meteorological, seeing, etc.).

The opening/closing of a shelter shall be controlled by Paranal weather services, assisted by a sky brightness monitor (diode).

5.2 Field orientation, Observing schedule

The camera will be zenith-centered, or pointed a few degrees south-west of zenith. Thereby, almost all VLT observations will be performed within the ASI field of view, and during one year, the full southern hemisphere will be covered. No scheduling *per se* is foreseen; the instrument shall function autonomously, and always view the same declination, hour angle (but see below).

5.3 Mounting

Considering the indicated resolution, typically $2'$ and the suggested exposure time, 5 seconds, stellar images will be slightly elongated, if the camera is mounted fixed. Photometric accuracy will be improved, if an equatorial mount is selected. The mount will reset between each single exposure, or between m exposures. If $m = 2^n$, that will allow simplified schemes of image stacking, for such applications, where lower time resolution is adequate, or where higher s/n-ratio must be obtained.

Also, the pre-calculation of input catalogue star observables (centroids and magnitudes, in dependence of refraction and extinction), will be eased, since it shall be repeated m times less often. In that case, the maximum duration of the observation is defined by the requirement that differential refraction across the $70°$ diagonal, shall not degrade detectability. Assuming maximum allowed differential refraction to be $6''$, implies 8 minutes of observation, or $m = 16$ series of B, V, R-exposures (see below).

A second, strong reason for a freely presetting mount (although not necessarily *tracking*) stems from flat-fielding requirements (see below).

5.4 Flat field exposures

Flat-fields will be generated by observation of the sky-background. As this has a zenith-distance component, it will be necessary to disentangle that from detector sensitivity through occasional observations taken in different directions, typically separated by 20 - 30°. Even then, it is not easy to generate the true detector sensitivity map; both (diffuse) sky background, and stellar intensities may have to enter the solution.

5.5 Need of shutter

Some chips can be used in frame transfer mode. However, it is rated that any such device is better used, if the full area is used for imaging. The disadvantage is that a (heavy duty) mechanical shutter has to be used, and that integrations cannot be performed during image read-out.

5.6 Filter wheel

A colored, optical filter can be inserted behind the optics, either on a wheel, or a slide. The filter, as well as the detector housing window has to enter the calculation of the optics. As mentioned above, it will be possible to correct some chromatic aberrations, using non-planar color-filters.

Neutral density filters may be provided, in order to extend operation into twilight hours.

5.7 Detector cooling

Long service intervals (weeks) are desirable, both for reason of operational costs, but also for stability of operation. It is therefore preferable to house the detector in a Peltier-cooled housing. The less deep cooling achieved this way, compared to cryogenic cooling, is justified by the short exposure times needed.

5.8 Lunar-occultor

As already mentioned above, a lunar-occultor may be needed. Indeed, "All Sky Monitors" at other facilities have found it desirable to shield Moon (and Sun), either with an non-transparent or a partially transparent occultor[6].

5.9 Integration time, Limiting magnitude

The integration time shall preferentially be so long that the read-out noise does not dominate over sky signal. The maximum integration time is defined from the need that jet-contrails are not smeared by much more than their extent. Moving at speeds of typically 30 m/s from West to East (hence approximately orthogonal to the flight direction), and seen from distance of minimum 7 km, the zenithal, angular speed is as large as $15'$ per second. The contrail width is initially typically 40 meters (the wing-tip distance), and rapidly increases to $\sim$100 meters. The cylindric rotation can remain stable for several km behind the aircraft. Eventually, the stable rotation dissolves, and the trail fades from visibility. However, under conditions of atmospheric supersaturated water vapor the contrail may grow virtually unlimited, and develop into regular clouds. In the early phase, which concern us here, the contrail will drift past the telescope field-of-view in a matter of seconds. To best detect the trail, using the ASI, will therefore require similarly short exposures.

Limiting magnitude: A very early calculation of the limiting magnitude is given in the Appendix A.

6 Data processing

6.1 Input Catalogue

Most likely, it will be found useful to employ an input catalogue. Thereby, the stars, which will be used to define the sky transmission, can be selected to have no known variability. Also stars of atypical (blue) colors can be excluded, hence improving the accuracy of pre-calculated atmospheric extinction. Alternatively, the catalogue can be bootstrapped from ASI observations, but that process will only complete after almost one year.

For the assistance to the VLT operations, the grid of standard stars shall be approximately uniform over the sky; no significant advantage is obtained from the larger density of stars available at low galactic latitudes. The first version of the Tycho catalogue[34] has approximately five stars per square degree to B=11.8, at the galactic poles. Almost all Tycho stars also have a V-magnitude. For the 70° x 90° field, some 33,000 stars will be measured. Some 10% of these will be rejected, for reason of color or variability. As each star in spread over $\sim$4 x 4 pixles, and the sky level has also to be measured, the full data analysis will involve some 30,000 x 100 pixels = 3.0 million pixels. This routine shall complete within 10 seconds, the basic cycle. The Sextractor software, as currently installed at ESO, handles 500,000 pixels per second, hence fully suitable to the needs of the ASI.

6.2 Detection of elongated objects (meteors, airplanes, satellite trails)

Given the above observing strategy, airplanes, satellites, meteors, near-earth objects, and other moving objects will be visible in the images as elongated trails if their proper motion is higher than about $1'$/s. Objects slower than that will be visible due to their motion in consecutive images only. Since such objects are not in the input catalogue they will not be detected in the reduction mentioned above. While the eye is an efficient detector for elongated objects on a starry background, it does cost some effort to recognize the streaks digitally. Special routines will work on difference images, $I = I_0 - 0.5*(I_- + I_+)$ where the vicinity of all stars have been masked out. If the positively deviating pixels are arranged along a line, this may be an indication of a moving object. Image profile analysis will reject cosmic-ray impacts.

6.3 Classification of elongated objects, contrail detection and forecast

Based on their characteristics, in particular regarding angular velocity, it should be straightforward to classify elongated objects into aircraft, meteors, satellites, or near-earth objects. This information should be used to veto any photometric information derived from stars in the vicinity of the proper great-circle segment. In the presence of very bright meteors, or satellite glints, it may be necessary to reject the entire ASI frame.

Assuming that an aircraft is detected, a special routine may test the photometric signature of an exhaust contrail (higher/lower sky background, lesser transparency). If so found, its sweeping motion over the sky can be predicted, in dependence of upper-atmospheric winds, and warnings issued to the VLT observer.

6.4 Contour plots of extinction, sky brightness

Once the ~30,000 stellar magnitudes have been calculated and compared to the expected magnitudes (in dependence of zenith distance and color), a contour plot can be made, presenting the relative transmission of the sky. This is the prime product of the ASI. In the absence of clouds, a more precise algorithm will calculate extinction coefficients (which is then assumed to have only low-frequency component in space and time). The high-level calculations put no further constraint on the computing speed, but will probably best be delegated to a separate processor.

Similar plots will be produced, showing the night-sky brightness. All maps will be tagged by the current locations of the various VLT unit telescopes, and the observer will be given the option to replay a sequence of earlier maps in time compressed mode.

At low galactic latitudes, source confusion will make it impossible to fully separate the atmosphere's contribution to the sky background.

6.5 Operational problems

- The need for pointed flat-field observations;
- Appearance of fireballs outside field-of-view;
- Strong satellite glints outside field-of-view;
- Local, man-made light-pollution (cars!);
- Dust accumulation on optics, need for frequent cleaning;
- Operation of a lunar occultor;
- ... and much, much more.

6.6 Data storage for service operations

No original data needs to be kept, only the contour maps, and the parameters of the possibly disturbing events.

7 ASI science opportunities

The ASI will be one of very few super wide-angle set-ups. Examples of somewhat similar systems are: APT[8], EROS[9], LINEAR[7], LONEOS[10], LOTIS[11], MACHO[12], ODAS[13], OGLE[14], ROTSE[16][17], and Spacewatch.[18] All have shown remarkable success within their particular field (near-earth objects, supernovae, gamma-ray bursts, microlensing events). These instruments, however, have a smaller field-of-view, compared to ASI, and thus do not capture the rarest events. Nemiroff and Rafert (1998) have described the desirability of a continuous record of the sky, and exemplified that with 4 k x 4 k CCD detector, capable of reaching magnitude 15.

The ASI will provide a valuable means of monitoring thousands of catalogued variable stars to 12th magnitude (or fainter, if image stacking can be employed, before image analysis). The photometric accuracy will not be very impressive, but the data will gain through the very high rate of repetition. Programming this function will not add excessively to that of the service function, since the positions of the variable stars are known a priori. Additionally, it can be expected that the ASI will detect a large number of new variable stars. There will also be occasional detections of objects of high proper motion. The advantage results partly from its location in the southern hemisphere, partly from its extreme field of view, and to some extent also from its high rate of repetition.

7.1 The variable sky

Apart from the totally unexpected, we can group the potential science functions into the following categories:

- *Comets*

  Figure 1a gives the frequency of comet discoveries, since January 1997, as function of declination (total: 42). Sun-grazing comets were excluded. Included in this statistics are the 12 comets found during 1998, with LINEAR[7] (this instrument has a main-mirror of 1-m diameter, and a 2560 x 1960 pixel detector), and some other instrumental discoveries. The deficiency of comet discoveries at southern declinations can be explained by the lesser number of southern observers, - and by the galactic bulge, which may be avoided by some visual observers. Figure 1b shows the brightness distribution. While not in itself indicative of gross systematics at bright magnitudes, some comets are undoubtedly missing, as revealed by a similar number ($\sim$39) of sun-grazing comets discovered during the same period, when already close to the sun. The recent visual finding of a m=9 magnitude comet[37] at declination $-69°$ corroborates this.

  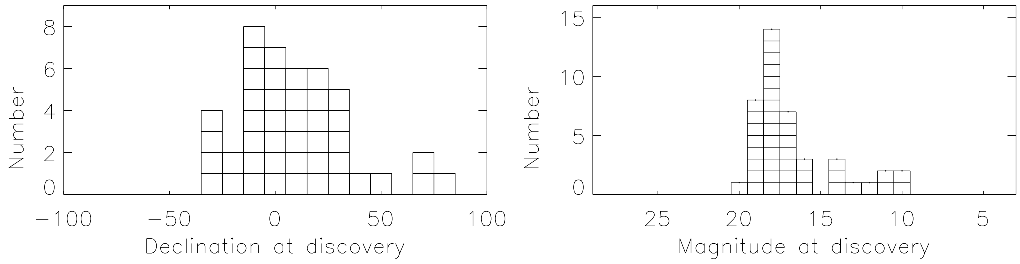

  Figure 1: Data for 42 comets (excluding Sun-grazing), discovered from January 1997 through February 1999: a: Declination at discovery; b: Magnitudes at discovery.

  With ASI, automatic detection of comets should be possible, in particular in the B-band.

- *Meteors and Fireballs*

  Similar to comets there is a large deficiency of permanent meteor streams at southern declinations: although about 25 main meteor streams are known, only 5 streams have a radiant with declination $< 0°$. This fact can to some extent be explained by the smaller number of southern observers. If operating for several years the ASI could detect new meteor streams.

  There exists also a not negligible possibility to register meteor showers of duration some hours only, similar to the phenomenon observed in the year 1946 in connection with comet Giacobini-Zinner. Besides, the hourly rate of sporadic meteors as well as the investigation of their diurnal and annual variation could improve the value of the daily mass of meteoric material reaching the Earth being now about 10 tons for high speed meteors.

  If a similar station as ASI at Paranal would operate also at La Silla, the simultaneous observations of meteors from two stations would enable us to determine their trajectories in the Earth's atmosphere, and in case of fireballs reaching the surface to determine the respective place of the impact. In the best case it would be possible to find the respective meteorite, which fact would be extremely valuable mainly for the physics of meteors. For obvious reasons, such investigations will be handled by Chilean scientists.

  The large field of view of the proposed ASI project would be very suitable in order to register the meteors, which would be distinguishable from other moving objects due to their light-curves and large angular velocities (several degrees/sec with the exception of very small areas close to the radiants).

- *Near Earth Objects, and asteroids in general*

  A 35 m diameter asteroid of type C would be visible[1] at the distance of the Moon, with a brightness near m(V) = 13.0. Following the estimate by Rabinowitz et al. (1993) that one 30-m object hits the Earth each year, it can be estimated that on a given day 10 boulders of this size pass closer to us than the Moon (Paczyński, 1996). About 1/5 of these will pass through the fov of the ASI, 1/3 at night time, 1/2 under no-Moon conditions, and 80/100 under clear sky conditions. Hence, unless the objects are smeared due to angular motion (which they generally are), we can estimate that NEO-observations will be made at a rate of two per week. Many of these observations will represent discoveries.

  It might be recalled that the 300-m asteroid 1996 JA1 passed just ∼453,000 km from the Earth, reaching magnitude 11 (Spahr, 1996). Some other significant NEO-events were: the record close passage ∼105,000 km of 1994 XM1, the 150,000 km passage of 1993 KA2, and the 170,000 km passage of the 5-10 m diameter object 1991BA (Scotti et al. 1991). Finally, New Scientist, on February 27, 1999, reported the discovery by LINEAR, of a 50-m asteroid in almost circular heliocentric orbit close to the Earth.

  Any similar discoveries by the ASI will not only be of interest scientifically, but also to the public. Observations by the ASI would improve the statistics of minor bodies in the Solar system, in particular in the poorly explored size regime from 1 to 500 m diameter.[46]

- *Detached eclipsing variables.*

  Paczyński (1996) has described detached eclipsing binaries as one of many fields in astronomy, which would benefit much from all-sky massive variability searches. These objects are the prime source of information on stellar masses, radii, and luminosities. It has been estimated that one out of 300 stars is a member of an eclipsing double star system.

  The Hipparcos mission showed that of the input catalogue of 118,204 stars (generally complete to H_p = 12.8) 8254 were variable, most of which new. Of the variables, 2712 were periodic, but it is not possible to say how many owe their variability to binary motion.

  The regular, and frequent photometry provided by the ASI will greatly facilitate the search for long-periodic eclipsing variables.

- *Semidetached eclipsing binaries (Algols)*

  Paczyński (1996) has pointed out that there are several strong selection effects in our knowledge of Algol systems. Most interesting is perhaps the notion that long-periodic Algol systems are much more frequent among bright stars ($m < 5$) than among faint stars ($9.5 < m < 10.0$) listed in the 4th General Catalogue of Variable Stars.[36]

  The ASI will serve to fill this gap.

- *Contact binaries (W Uma, RS CVn)*

  As pointed out by Paczyńsky (1996), the inventory of these classes of objects suffers from incompleteness, also at the fairly bright magnitudes available to the ASI.

- *Single, spotted stars (Ap-stars, He-variables)*

  Ap-stars and He-variable stars are young stars, believed to have a fracctionated stellar wind, leaving the surface enriched/depleted in certain elements. Rotation produces variability in spectroscopic absorption lines, and in broad-band photometry. The photometric variability can be up to 0.1 magnitude.[43]

- *Pulsating stars (Miras, Cepheids, RR Lyrae, δ Scuti)*

  These objects have amplitudes of 1 magnitude, typically, and the periods range from several hours to months. The sky is incompletely mapped, with a notable absence of sources fainter than m ∼10.

  The ASI would provide a wealth of data on known and new pulsating stars.

[1] A large fraction of asteroids, 75%, or more, are of this low-albedo "carbonaceous" type, and remainder of the brighter "silicaceous" and "metallic" types.

- *Flare stars (dMe stars)*

  Some flare stars exhibit 0.2 - 1.5 flares/hour (Pettersen, et al., 1986). The brightest known flare star, UV Ceti, has a quiescent brightness near $m_U = 14.6$, $m_B = 13.5$, and $m_V = 12.0$, and the flare amplitude can reach $\Delta m_U = 6.5$, $\Delta m_B = 4.3$, $\Delta m_V = 3.2$ magnitude[39]. This object and undoubtedly many other flare stars will be visible by the ASI, either in quiescence, or in outburst.

- *Novae*

  Galactic novae are found at a uniform rate of about 6 per year. Most rise by 10 - 11 magnitudes, some by 20, to $m < 12$, at maximum.[54] The distribution is strongly concentrated along the galactic plane. It has been pointed out that some novae as bright as magnitude 4 - 6 seem to pass undetected, and that few have been caught on the initial rise; fragmentary data suggest that the rise from pre-nova level to two magnitudes below maximum takes place within 2 to 3 days, even in the case of *slow novae*.[33]

  The recent case of nova Velorum 1999, discovered at m(V) = 3.1 underlines the potential role of the ASI, for locating novae while still on the rise.

- *Dwarf Novae (U Gem), Recurrent Novae*

  Dwarf Novae are repeating novae, having quasi-periodic outbursts, with intervals of weeks or months. The flaring amplitude is typically 3 to 7 magnitudes. One of the best know dwarf novae, SS Cygni, increases from 12.1 to 8.1 mag. Recurrent Novae are much rarer objects, with amplitude 8 - 10 mag. The prime example is T Cor Bor, which underwent outbursts in 1866 and 1946.

  The ASI would serve to call attention to such outbursts at an early moment, hence permitting follow-up at larger facilities.

- *X-ray Bursters, X-ray Transients, persistent X-ray stars*

  The two first classes of objects include low-mass binaries, with a mass-receiving neutron-star. In general they are too faint to be seen by the ASI. Some other, persistent X-ray sources, like the black-hole candidate Cyg X-1 (m=8.9 with 0.1 mag oscillations) can easily be monitored.

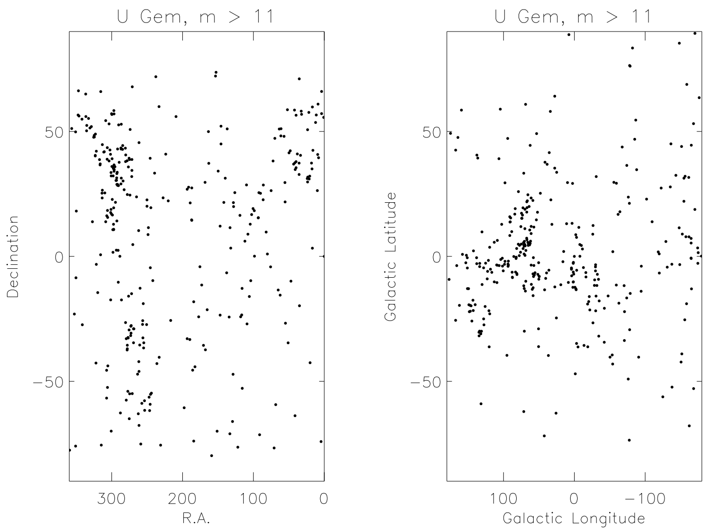

Figure 2: The celestial distribution of dwarf novae stars (type U Gem), fainter than magnitude 11: in equatorial coordinates (a) and in galactic coordinates (b). The distribution is patchy, and biased towards the northern hemisphere, reflecting the catalog's incompleteness.

- *X-ray Novae*

  X-ray Novae are galactic objects, and strong black hole candidates. Examples are Nova Muscae 1991[32] ($m=20 \rightarrow 13$), A0600−20 ($m=20 \rightarrow 10.4$), GS 2000+25, GRO J0422+32.

  The ASI will record several of these objects, when in outburst.

- *Extreme UV transients*

  The ALEXIS satellite[19] detects an "Extreme UV Transient" at a rate of one per week. More may be forthcoming, from the recently launched ARGOS satellite.[26] The (reality and) nature of these events is unknown; confirmation from ground-based observations would be highly desirable.

- *Microlensing events*

  Microlensing is an astrophysically interesting phenomenon, capable of revealing physical properties of stars. Any galactic star has a chance of less than one in a million, of being amplified, due to gravitational lensing by another star. Caustic crossings of double stars may cause very high, 'singular', magnification. Several large surveys, OGLE, MACHO, DUO, EROS, monitor huge numbers of stars (25 million, in the case of OGLE[52]). Among the many events found so far (some 300 in the galactic bulge region [28], and similar in the LMC, [29]), some show evidence for duplicity (see e.g. [47]), and one claim has been made for the detection of a planetary companion[48]. This latter event was noticeable also for the record magnification factor ~80. At least one, well-documented gravitational lensing event was marginally bright enough to be detected by the ASI; its quiescent brightness was m = 12.9, and the amplitude Δm = 0.22 mag.[15]

- *Quasars and other active galactic nuclei*

  The quasar 3C273 varies between magnitude 12.8 in (relative) quiescence, to 11.7 in light maximum. Some of the brightest AGN, and their variability ranges are BL Lac (17.2 $\rightarrow$ 12.4), W Com (17.5 $\rightarrow$ 11.5). In their maxima, they, and undoubtedly several other AGN will come into view by the ASI.

- *Supernovae*

  Three or 4 supernovae, annually, reach 14 magnitude, or brighter.[20] This number has been approximately constant, since ~1960, indicating a high degree of completeness within the set of galaxies surveyed. Most supernovae are discovered while already declining in brightness. Photometry on bright supernovae is still often done visually. For the brightness interval $12 < m < 14.5$, the typical accuracy of such estimates is 0.3 magnitude.[53]

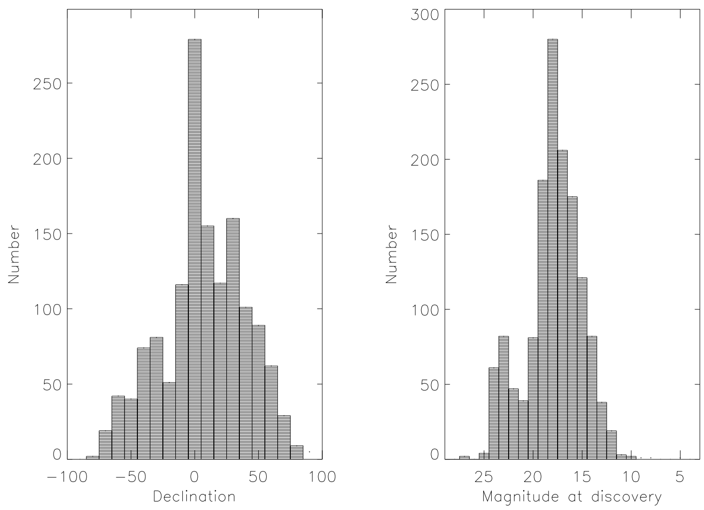

Figure 3: Data for 1431 supernovae, discovered 1900 through February 1999: a: Declination; b: Magnitudes at discovery. The galactic bulge may be partly responsible for the low rate of supernovae discoveries near δ $-25°$. The bimodal nature of the magnitude distribution is due to recent success with automated detection procedures, using large telescopes, including HST.

For supernovae of type Ia, Paczyński (1996) has estimated that the whole-sky rate is

$$N \sim 300 * 10^{0.6(m_{max}-17.0)} \text{ yr}^{-1}$$

Hence, if a limiting magnitude of $m \sim 14$ can be achieved from the ASI, by image-averaging, then up to three such events can be recorded annually. The ASI will be able to document some supernovae, while they are still rising. At discovery, SN1987A was seen as an object nof 5th magnitude and could potentially have been detected hours earlier, with an instrument like ASI.

- *Optical Transients from Gamma Ray Burst sources*

  OTs are entirely feasible discoveries, as revealed by the recent case of GRB990123 (at redshift z = 1.6), for which the optical counterpart for some seconds reached 9th magnitude.[30]

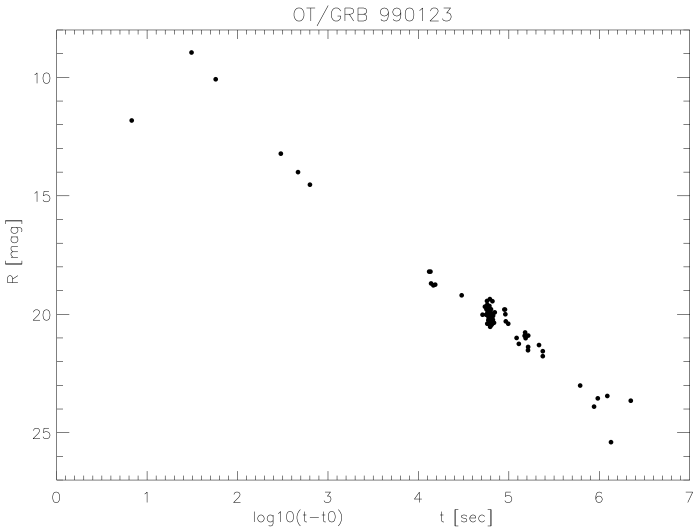

Figure 5: Photometry of the Optical Transient from GRB990123, combined from various sources (GCN circulars, IAU Circulars, and unpublished NOT observations). The early optical observations were obtained using a quickly presetting telescope, the ROTSE instrument of Los Alamos National Labs.[16] The horizontal scale shows time-difference since BATSE trigger t0.

It is interesting to speculate that some of these potential detections might be done independent of the high-energy detection. Although schemes are in operation to search for OTs while GRBs are in progress (ROTSE, LOTIS, TAROT[21]), these rely on data transmission from space, hence an assumption that optical emission can be detected several seconds after the start of the GRB. Little is currently known about optical transients from short-lasting GRBs; these may only be visible optically, if observations are done in strict simultaneity.

- *Soft Gamma Repeaters*

  The generally accepted model is that of *magnetars*, i.e. young neutron stars undergoing some form of event in a super-strong (10^{15} gauss) magnetic field.[27] There are only four of these sources known, two of which are known as pulsars.[35] The events occur over a range of time scales, and periods of activity may be followed by years of inactivity. With one exception all SGRs are galactic, and placed behind many magnitudes of dust absorption. The exception is SGR 0526-66, source of the famous March 5, 1979 event, located in the N49 supernova remnant in the LMC. There are unconfirmed observations of 9th magnitude optical flashes from this object.[42] Continued monitoring at time resolution $<$ 10 seconds is required to test this discovery when and if the source enters a second period of activity.

- *Gravitational Wave Events*

  No such event has ever been confirmed, but the forthcoming LIGO [22] and VIRGO [23] gravitational wave detectors will greatly increase sensitivity. When operational, need may therefore arise for all-sky, continuously operating optical detectors. It should be recalled that several models, which have been proposed as sources of gravitational waves, are also invoked to explain gamma-ray bursts.[31]

- *UHE cosmic ray events*

  The nature of these events, having energies at least to 3.2 10^{20} eV, is not clear.[24] Associated optical observations may provide a clue. Wide angle detectors are required, since the events are located to no better than 2°.

- *Neutrino detections*

  Existing neutrino detectors are much more sensitive than those which registered the 20 neutrinos from SN1987A. It would be desirable that future neutrino detections are checked against a data-base of all-sky images; the large solid-angle coverage by ASI could thus prove valuable.

- *Sky Brightness*

  The full hemisphere monitoring of the night sky brightness all year around is another exciting scientific database. Could there be other diffuse, low-surface brightness sources than the Gegenschein? Recall the discovery of a Sodium cloud trailing the Moon during the 1988 leonid display[25].

7.2 Software for science operations

Full-frame data analysis will exceed that required by the ASI prime function by one to two orders of magnitude. While feasibility in terms of computing speed still has to be demonstrated, much of the software should be available from the ESO Imaging Survey (EIS) project, and further assistance can probably be had from some of the abovementioned survey programmes. This includes software to recognize streaks in individual exposures, objects moving from frame to frame, automatic generation of ephemeris for such objects, etc.

7.3 Data storage for science operations

The full data rate of the ASI, ~150 TB/year, exceeds the total output of the entire VLT operations. This will present problems for data archiving. Accordingly, we will consider the possibility to make a full inventory each exposure cycle, or each m exposures, and archiving only the photometric output tables, or the potentially interesting entries.

Partial or full frames may be kept for later off-line analysis, if real-time alerts have arisen, e.g. from the existing missions BATSE, BeppoSAX, Ulysses, ALEXIS, or the forthcoming missions INTEGRAL, HETE-II, and others. Information on ground-based discoveries may be decoded from IAU Circulars, and other dependable sources, and used to trigger automatic storage of selected image portions.

After an initial period of linear growth lasting almost one year, the size of the archive will grow as the logarithm of time. Reference frames can be built up, which shows the sky at successively longer time-scales.

7.4 Data visibility

It is desirable, that tables on discoveries are made readable on the world wide web.

8 Time schedule

- Design
- Construction
  - Optics
  - CCD housing
  - Filter/Shutter
  - Mount
  - Housing
  - Software for ASI service functions
  - Software for ASI scientific data analysis
- Assembly

9 Participating institutions

10 Acknowledgments

We are grateful to L.Kohoutek, Hamburg, for having drafted the section on meteors and fireballs, and to C.I.Johanesson, Uppsala, for reviewing the section on asteroids and comets.

References

[1] "Scientific Requirements to a VLT All Sky Monitor", 1998, http://www.eso.org/gen-fac/pubs/astclim/contrails/contrail-monitor-1098.ps.gz

[2] "Humidity and Cirrus Cloud Cover Forecasts for ESO Observatories at La Silla and Paranal", http://www.eso.org/gen-fac/pubs/astclim/forecast/meteo/ERASMUS/

[3] "Anthropogenic Effects on Observing Conditions at Paranal", 1997, http://www.eso.org/gen-fac/pubs/astclim/contrails /contrail-070597.ps

[4] http://www-mpl.ucsd.edu/people/jshields

[5] http://vega.bu.edu/planetary/mcdonald.html

[6] http://WWW.ARM.GOV./docs/instruments/static/wsi.html

[7] http://www.ll.mil.edu/LINEAR

[8] http://www.phys.unsw.edu.au/~mcba/apt.html

[9] http://www.lal.in2p3.fr/EROS/erosa.html

[10] http://www.lowell.edu/users/elgb/loneos_disc.html

[11] http://hubcap.clemson.edu/~ggwilli/LOTIS/

[12] http://wwwmacho.mcmaster.ca/

[13] http://pentium.pe.ba.dlr.de/odas/odas.htm

[14] http://www.astrouw.edu.pl/~ftp/ogle/index.html

[15] http://www.astro.princeton.edu/~ogle/OGLE2/ews/bul-12.html

[16] http://www.umich.edu/~rotse

[17] http://www.umich.edu/~rotse/rotse-ii/rotseii.html

[18] http://pirlwww.lpl.arizona.edu/spacewatch/

[19] http://gcn.gsfc.nasa.gov/gcn/alexis_trans.html

[20] http://cfa-www.harvard.edu/iau/lists/Supernovae.html

[21] http://www.cesr.fr/~boer/sursauts-XMM/grb/etarotind.html

[22] http://www.ligo.caltech.edu

[23] http://virgo4p.pg.infn.it/virgo/

[24] http://www.physics.adelaide.edu.au/astrophysics/3e20.html

[25] http://vega.bu.edu/moontail/

[26] http://www.te.plk.af.mil/arpics/apage4.cfm

[27] http://science.msfc.nasa.gov/newhome/headlines/ast20may98_1.htm

[28] Alcock, C., et al., 1999, "Difference Image Analysis of Galactic Microlensing II. Microlensing Events", astro-ph/9903219

[29] Alcock, C., et al., 1999, ApJ, 518, 44-49.

[30] Akerlof, C., and McKay, T.A., 1999, "GRB 990123", IAU Circular No. 7100.

[31] Brown, G.E., et al., 1999, astro-ph/9905337.

[32] Della Valle, M., et al., 1991, in IAU Circular Nos. 5165 & 5167.

[33] Duerbeck, H.W., 1990, "Galactic distribution and outburst frequency of classical novae", in *Physics of Classical Novae, Lecture Notes in Physics*, Eds. A.Cassertella and R.Viotti, Springer Verlag, p.34.

[34] ESA, 1997, "The Hipparcos and Tycho Catalogues", ESA SP-1200

[35] Feroci, M., et al., 1999, "A Giant Outburst from SGR 1900+14 Observed with the BeppoSAX Gamma-Ray Burst Monitor", ApJL, 515, L9.

[36] Kopolov, P.N., et al., 1988, General Catalogue of Variable Stars, 4th Edition, Moscow.

[37] Lee, S., 1999, "Comet 1999 H1", in IAU Circular No. 7144.

[38] Lesser, M., et al., http://sauron.as.arizona.edu/ccdlab/projects/7kx9k/7kx9k_paper.html

[39] Melikian, N.D., 1984, http://www.konkoly.hu/pub/ibvs/2601/2630.txt.

[40] Nemiroff, R.J., & Rafert, J.B., 1998, "Towards a Continuous Record of the Sky", astro-ph/9809403

[41] Paczyński, B., 1996, "The Future of Massive Variability Searches", http://a188-1009.rit.edu/tass/refs/searches.ps

[42] Pedersen, H., et al., 1984, "Detection of possible Optical Flashes from GBS 0526-66", Nature, 312, p.46.

[43] Pedersen, H., & Thomsen, B., 1977, "Spectrum and photometric variability of He-weak and He-strong stars", Astron.Astroph.Suppl.Ser. 30, p.11.

[44] Pettersen, B.R., et al., 1986, "Analysis of the flare activity of AD Leo", Astron.Astroph.Suppl.Ser. 66, p.235.

[45] Rabinowitz, D.L., et al., 1993, "The size distribution of the earth-approaching asteroids", Astrophys.Journ., 407, p.412.

[46] Rabinowitz, D.L., 1997, "Are Main-Belt Asteroids a Sufficient Source for the Earth-Approaching Asteroids?", Icarus 130, 287-295.

[47] Rhie, S.H., 1999, astro-ph/9903024

[48] Rhie, S.H., Bennet, D., et al., 1999, AAS Meeting #193, #108.05

[49] Scotti, J.V., et al. 1991, "Near miss of the Earth by a small Asteroid", Nature, 354, 287.

[50] Spahr, T., 1996, "1996 JA1", in IAU Circular 6402.

[51] Theuwissen, A.J.P., Beletic, J.W., & Amico, P., 1999, preprint.

[52] Udalsky, A., et al., 1999, "OGLE-2 system for microlensing events", in IAU Circ. No. 6901

[53] Vinko., J., et al., 1999, astro-ph/9903138

[54] Warner, B., 1989, "Properties of novae: an overview", in *Classical Novae*, Eds. M.F.Bode & A.Evans, J.Wiley & Sons Ltd., p.1.

11 System parameters

The following is a trial calculation of the sensitivity of the Lockheed-Martin chip, mounted behind a 4 cm focal length lens of effective aperture 2.8. The field size is calculated assuming gnomonic projection.

```
VLT All Sky Imager
==================

Calculation of limiting magnitude for "empty" pix

The camera optics is assumed to produce a uniform illumination
of n (see below) pixels, each of which exceeding sky by
sigma (see below)

The estimate of optics transmission includes  exclusively
color filter and dewar entrance window (0.94), while
other losses are taken into account by means of the f-ratio


  SKY AND BANDPASS:
  Flux  V=0 A0 star @ ctrl wvl [erg/cm2/s/A]    6.76000E-09
  Central wavelength [A]                            5400.00
  Bandwidth [A]                                     1500.00
  Filter transmission                              0.850000
  Sky background magnitude []                       21.9000
  Extinction coefficient, p                        0.200000
  Airmass, z                                        1.10000

  CCD:
  Pixel size [mu]                                   8.75000
  Quantum efficiency                               0.400000
  Charge-well capacity [e-]                        100000.0
  CCD read-out noise [e-]                           15.0000
  Number of pixels in each dimension          9000 *  9000

  EXPOSURE:
  Exposure time [s]                                10.00000
  Significance requested, n x sigma          16    2.00000

  TELESCOPE:
  Diameter of aperture [cm]                         1.42857
  Diameter of central obscuration [cm]                   0.

  PERFORMANCE:
  Focal length of optics [cm]                       4.00000
  f ratio, effective                                2.80000
  Pixel size [asec]                                 45.1205
  Field-size [degrees]                 89.0977 *    89.0977
  Time for sky to saturate charge well [s]          24408.9
  Saturation magnitude, uniform distrib []          2.14896
  Limiting magnitude  []                            11.7115
```